Chapter 3

Voltage Stability Estimation of Real Time Systems Using Phasor Measurements

3.1 Introduction

Maintenance of voltage stability has been considered to be a major challenge for researchers and utilities since last few decades. Severe incidences of grid collapse initiated by voltage instability have been observed in different parts of the world [78]. Most of the research has concentrated on offline estimation of voltage stability margin. A fast and accurate methodology is required for voltage stability monitoring and control of real time systems. The use of Phasor Measurement Unit (PMU) technology in monitoring, control and protection of power systems is well documented [33]. PMU measurements may be quite useful in voltage stability estimation of real time systems.

Voltage stability estimation based on PMU measurements may be mainly classified as methods based on Thevenin's equivalent of power system about critical bus [32], [100-101] defining voltage stability index using Tellegen's theorem [102] and sensitivity based approaches [36], [103-104]. However, these methods consider linear approximation of power system network which is not valid near stressed point. A voltage stability index utilizing data obtained from phasor measurements is used to find critical buses, and a new parallel optimization method has been used to increase voltage stability margin of the system [105]. A local autonomous protection against voltage instability has been developed that generates alarm in case of voltage being unstable [106]. A measurement based voltage stability monitoring method for a local area fed by tie line is proposed [107].

Continuation power flow method has been shown to be an accurate approach for voltage stability estimation of offline systems [10], [108]. Nose curves may be accurately obtained from continuation power flow method, and maximum loadability of the system may be found, there from. However, being computationally involved, continuation power flow method may not be suitable for voltage stability estimation of real time systems. An approximate fitting of nose curves using quadratic approximation has been proposed [109]. Quadratic curve fitting proposed in [109] considers two step continuation power flow. Global parametric polynomial approximation of static voltage stability region boundaries has been proposed [110]. However, polynomial approximation proposed in [109-110] assumed static power system model which may not be suitable for real time systems.

In this chapter, quadratic curve fitting of nose curves based on phasor measurements obtained at the base case operating point and two higher loading points, has been considered. Simulations have been performed on Power System Analysis Toolbox (PSAT) software. In order to consider different operating scenario, nose curves have been estimated under critical contingencies and changing load patterns.

3.2 Proposed Approach for Voltage Stability Assessment

The loading factor (λ) versus bus voltage magnitude (V) curve (λ –V curve) may be computed using continuation power flow method utilizing predictor corrector steps as shown in Figure-3.1 [10]. Continuation power flow method though accurately determines the voltage stability margin, is a computationally involved algorithm, and this may not be suitable for voltage stability estimation of real time systems. The nose

point (maximum loadability point) of λ –V curve may be fast predicted by a generalized curve fitting method presented below:

The λ–V curve may be approximately obtained by solution of following equation:

$$\lambda = a_1 V^2 + a_2 V + a_3 \qquad (3.1)$$

where a_1, a_2, a_3 are constants.

Differentiating λ with respect to V,

$$\frac{d\lambda}{dV} = 2a_1 V + a_2 \qquad (3.2)$$

At the nose point of λ–V curve, $\frac{d\lambda}{dV}$ =0. Therefore, from (3.2),

$$V_n = -\frac{a_2}{2a_1} \qquad (3.3)$$

where, V_n is the bus voltage at the nose point.

From (3.1) and (3.3),

$$\lambda_{\max} = -\frac{a_2^2}{4a_1} + a_3 \qquad (3.4)$$

where, $\lambda_{\max}$ is the loading factor at the maximum loadability point, and represents voltage stability margin of the bus. The constants a_1, a_2, a_3 may be obtained by solution of equations:

$$\lambda^1 = a_1 (V^1)^2 + a_2 V^1 + a_3 \qquad (3.5)$$

$$\lambda^2 = a_1 (V^2)^2 + a_2 V^2 + a_3 \qquad (3.6)$$

$$\lambda^3 = a_1 (V^3)^2 + a_2 V^3 + a_3 \qquad (3.7)$$

where, 1, 2, 3 represent three different points of λ–V curve. Base case operating point ($\lambda=0$) may be considered point 1 whereas, points 2 and 3 may be obtained by solution of two step continuation power flow method [109]. However, continuation power flow method is based on static approximation of power system, and it does not consider impact of dynamics of components such as excitation system and induction motors on variation of bus voltages at different operating points. Therefore, bus voltages determined at three different loading points by two step continuation power flow may not be valid for real time systems, and constants a_1, a_2, a_3 computed may lead to erroneous estimation of maximum loadability (λ_{max}). Present work proposes calculation of constants a_1, a_2, a_3 using measurement of bus voltage by Phasor Measurement Unit (PMU) at the base case operating point ($\lambda^1=0$) and two other operating points corresponding to λ^2 and λ^3 at increased loadings.

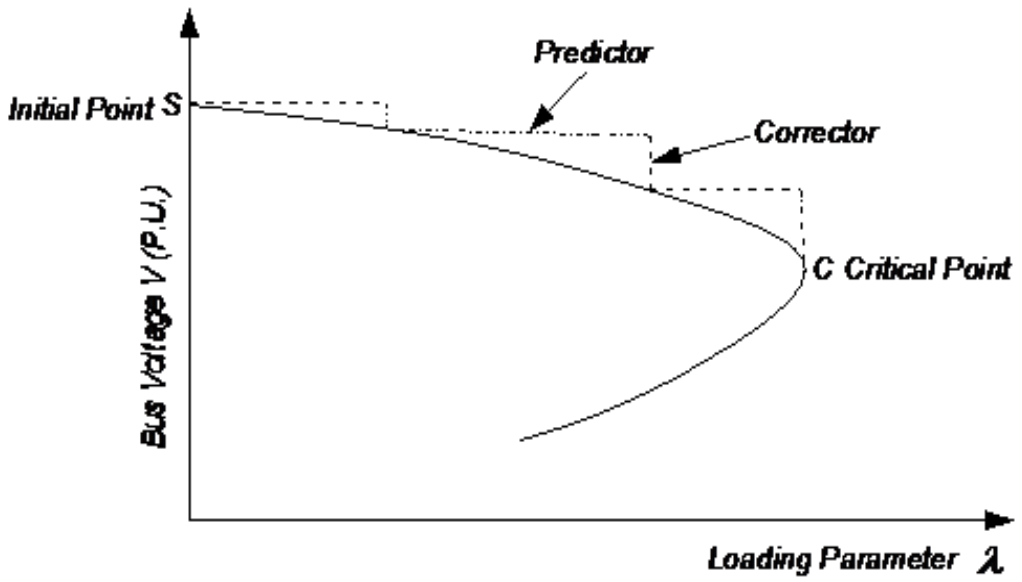

Figure 3.1: Nose curve (λ-V curve) obtained using continuation power flow method

3.3 Case Studies

Case studies were carried out on IEEE 14-bus system, New England 39-bus system and NRPG 246-bus system. Details of three test systems are given in Appendix-A, Appendix-B and Appendix-C, respectively. Simulation results of three systems obtained using PSAT software are presented below:

3.3.1. IEEE 14-Bus System

Nose curves (λ-V curves) of buses were obtained for the system intact case and all the single line outage cases under different patterns of load increase, using

Approach 1: running full continuation power flow

Approach 2: evaluating constants a_1, a_2, a_3 using phasor measurements obtained at three different operating points, and estimating nose curve by quadratic curve fitting. Base case operating point ($\lambda=0$) has been considered as point 1. Points 2 and 3 correspond to bus voltage magnitude of 0.95 p.u. and 0.90 p.u., respectively. Phasor information obtained from PMUs placed at bus numbers 2, 4, 5, 6, 9 as per Table 2.2 have been utilized to estimate nose curve by quadratic curve fitting.

Voltage magnitude of critical buses at the base case operating point with λ=0 (i.e. at point 1) have been shown in Table 3.1 for k=0.2 and k=0.5, respectively, and in Table 3.2 for k=1.0 and 1.2, respectively. Loading factor of critical buses corresponding to bus voltage magnitude of 0.95 p.u. (i.e. at point 2) have been shown in Table 3.3 for k=0.2 and k=0.5, respectively, and in Table 3.4 for k=1.0 and 1.2, respectively. Loading factor of critical buses corresponding to bus voltage magnitude

of 0.90 p.u. (i.e. at point 3) have been shown in Table 3.5 for k=0.2 and k=0.5, respectively, and in Table 3.6 for k=1.0 and 1.2, respectively.

Constants a_1, a_2, a_3 computed by Approach-2 (based on phasor measurements) have been shown in Table 3.7, Table 3.8, Table 3.9 and Table 3.10 for k=0.2, k=0.5, k=1.0 and k=1.2, respectively. Voltage stability margin (maximum loadability i.e. λ_{max}) obtained by two approaches have been shown in Table 3.11, Table 3.12, Table 3.13 and Table 3.14 for k=0.2, k=0.5, k=1.0 and k=1.2, respectively.

Loading factor versus bus voltage magnitude (λ-V) curve of critical bus 5 under line outage 1-2 for k=0.2, obtained by two approaches, have been shown in Figure-3.2. λ-V curve of critical bus 4 under line outage 2-3 for k=1.0, obtained by two approaches, have been shown in Figure-3.3.

It is observed from Table 3.11, Table 3.12, Table 3.13 and Table 3.14, and Figure-3.2 and Figure-3.3, that voltage stability margin estimated by quadratic nose curve fitting based on phasor measurements obtained at three operating points closely match with voltage stability margin estimated by full continuation power flow. However, it is observed from Figure 3.2 and Figure 3.3 that though bus voltage magnitudes at the base case operating point are same by two approaches, voltages obtained by two approaches differ at other operating points.

Critical contingencies as well as critical buses depend upon system dynamic conditions in case of real time systems. However, in order to compare voltage stability margin estimated by proposed approach with existing approach, critical contingencies have been obtained based on voltage stability margin (distance between the base case operating point and the nose point) computed by continuation power flow method.

Critical buses have been obtained based on sensitivity of bus voltage magnitude to loading factor (i.e. $dV/d\lambda$) computed near nose point of λ-V curve. PMU measurements have been obtained using PSAT software.

Table 3.1: Voltage magnitude of critical buses at point-1 (λ=0, k=0.2, 0.5)

Line Outage	Critical Bus No.	Bus Voltage Magnitude (p.u.)	
		k=0.2	k=0.5
		Approach-1 & Approach-2	Approach-1 & Approach-2
Intact Case	4	1.03	1.03
	5	1.03	1.03
1-2	5	1.03	1.03
2-3	4	1.03	1.03
	5	1.03	1.03
5-6	4	1.03	1.03
	5	1.03	1.03
	9	1.05	1.05
	14	1.05	1.05

Table 3.2: Voltage magnitude of critical buses at point-1 (λ=0, k=1.0, 1.2)

Line Outage	Critical Bus No.	Bus Voltage Magnitude (p.u.)	
		k=1.0	k=1.2
		Approach-1 & Approach-2	Approach-1 & Approach-2
Intact Case	4	1.03	1.03
	5	1.03	1.03
2-3	4	1.03	1.03
	5	1.03	1.03
5-6	4	1.03	1.03
	5	1.03	1.03

Table 3.3: Loading factor of critical buses at point-2 (*V*=0.95 p.u., *k*=0.2, 0.5)

Line Outage	Critical Bus No.	Loading Factor	
		***k*=0.2**	***k*=0.5**
		Approach-1 & Approach-2	**Approach-1 & Approach-2**
Intact Case	4	4.70	4.75
	5	3.72	3.76
1-2	5	1.31	1.29
2-3	4	2.67	2.53
	5	2.86	2.75
5-6	4	2.90	3.07
	5	4.01	3.89
	9	4.40	4.32
	14	4.06	3.74

Table 3.4: Loading factor of critical buses at point-2 (*V*=0.95 p.u., *k*=1.0, 1.2)

Line Outage	Critical Bus No.	Loading Factor	
		***k*=1.0**	***k*=1.2**
		Approach-1 & Approach-2	**Approach-1 & Approach-2**
Intact Case	4	3.84	4.86
	5	3.03	3.72
2-3	4	2.67	2.67
	5	2.86	2.69
5-6	4	3.11	3.11
	5	2.86	4.01

Table 3.5: Loading factor of critical buses at point-3 (*V*=0.90 p.u., *k*=0.2, 0.5)

Line Outage	Critical Bus No.	Loading Factor	
		***k*=0.2**	***k*=0.5**
		Approach-1 & Approach-2	**Approach-1 & Approach-2**
Intact Case	4	5.26	5.24
	5	4.54	4.59
1-2	5	1.33	1.34
2-3	4	2.97	2.98
	5	3.20	3.16
5-6	4	3.81	3.83
	5	4.44	4.48
	9	4.47	4.39
	14	4.89	4.76

Table 3.6: Loading factor of critical buses at point-3 (*V*=0.90 p.u., *k*=1.0, 1.2)

Line Outage	Critical Bus No.	Loading Factor	
		***k*=1.0**	***k*=1.2**
		Approach-1 & Approach-2	**Approach-1 & Approach-2**
Intact Case	4	4.64	5.26
	5	3.88	4.54
2-3	4	2.98	2.99
	5	3.20	3.20
5-6	4	3.95	3.95
	5	3.20	4.44

Table 3.7: Constants a_1, a_2, a_3 for k=0.2

Line Outage	Critical Bus No.	Evaluated Constants		
		a_1	a_2	a_3
		Approach-2	Approach-2	Approach-2
Intact Case	4	-412.7	615.2	-337.8
	5	-338.1	615.2	-275.3
1-2	5	-208.4	393.9	-184.7
2-3	4	-250.3	458.4	-206.9
	5	-236.6	430.2	-192.4
5-6	4	-226.7	405.8	-177.7
	5	-326.9	597.1	-268.1
	9	-393.2	742.7	-346.1
	14	-156.2	272.8	-114.0

Table 3.8: Constants a_1, a_2, a_3 for k=0.5

Line Outage	Critical Bus No.	Evaluated Constants		
		a_1	a_2	a_3
		Approach-2	Approach-2	Approach-2
Intact Case	4	-421.2	768.8	-345.4
	5	-318.2	576.4	-256.3
1-2	5	-225.6	428.0	-201.5
2-3	4	-267.7	491.4	-222.4
	5	-269.6	494.7	-223.7
5-6	4	-219.1	390.8	-170.4
	5	-337.0	615.9	-276.8
	9	-320.9	599.4	-275.3
	14	-138.6	239.6	-98.6

Table 3.9: Constants a_1, a_2, a_3 for k=1.0

Line Outage	Critical Bus No.	Evaluated Constants		
		a_1	a_2	a_3
		Approach-2	Approach-2	Approach-2
Intact Case	4	-584.0	1093	-506.9
	5	-227.1	406.5	-178.0
2-3	4	-265.7	488.2	-221.3
	5	-230.6	418.7	-186.8
5-6	4	-227.2	405.5	-176.8
	5	-208.4	377.8	-167.9

Table 3.10: Constants a_1, a_2, a_3 for k=1.2

Line Outage	Critical Bus No.	Evaluated Constants		
		a_1	a_2	a_3
		Approach-2	Approach-2	Approach-2
Intact Case	4	-469.3	862.5	-390.9
	5	-322.0	584.0	-260.3
1-2	5	-205.0	387.3	-181.5
2-3	4	-269.8	496.2	-225.1
	5	-259.9	475.1	-213.8
5-6	4	-219.4	390.7	-169.9
	5	-310.9	566.1	-253.2
	9	-278.6	517.1	-235.6
	14	-103.7	174.5	-68.7

Table 3.11: Voltage stability margin by two approaches for k = 0.2

Line outage	Critical Bus No.	Approach-1	Approach-2
Intact	4	5.26	5.33
	5	4.93	4.55
1-2	5	1.33	1.36
2-3	4	2.99	3.01
	5	3.34	3.21
5-6	4	4.46	3.84
	5	4.61	4.47
	9	4.93	4.56
	14	4.91	5.07

Table 3.12: Voltage stability margin by two approaches for k = 0.5

Line outage	Critical Bus No.	Approach-1	Approach-2
Intact	4	5.26	5.36
	5	4.93	4.60
1-2	5	1.34	1.36
2-3	4	2.99	3.10
	5	3.34	3.17
5-6	4	4.47	3.88
	5	4.61	4.56
	9	4.40	4.50
	14	4.90	4.96

Table 3.13: Voltage stability margin by two Approaches for k = 1.0

Line outage	Critical Bus No.	Approach-1	Approach-2
Intact	4	4.64	4.67
	5	4.29	3.88
2-3	4	2.94	3.02
	5	3.04	3.21
5-6	4	4.48	4.01
	5	4.61	3.21

Table 3.14: Voltage stability margin by two approaches for k = 1.2

Line outage	Critical Bus No.	Approach-1	Approach-2
Intact	4	5.26	5.33
	5	4.92	4.54
1-2	5	1.33	1.36
2-3	4	2.99	3.02
	5	3.34	3.25
5-6	4	4.48	3.97
	5	4.61	4.46
	9	4.22	4.30
	14	4.88	4.67

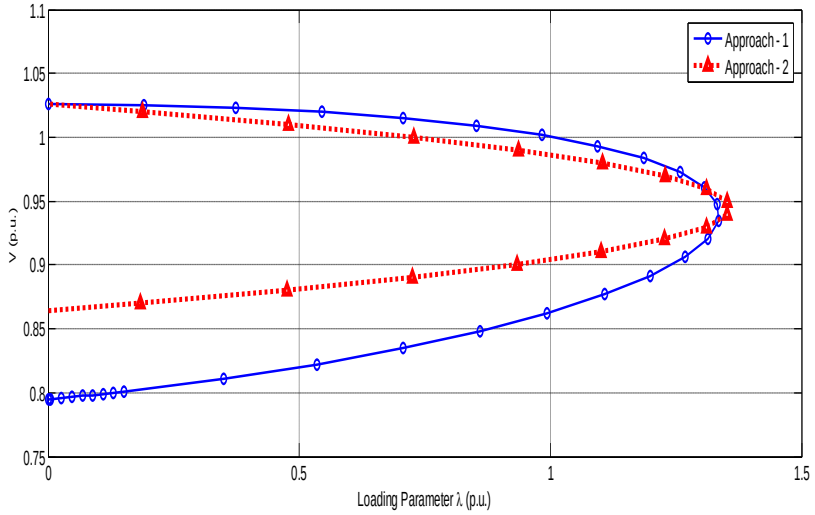

Figure 3.2: Nose curve of critical bus 5 under line outage 1-2 for *k* = 0.2 (IEEE 14-bus system)

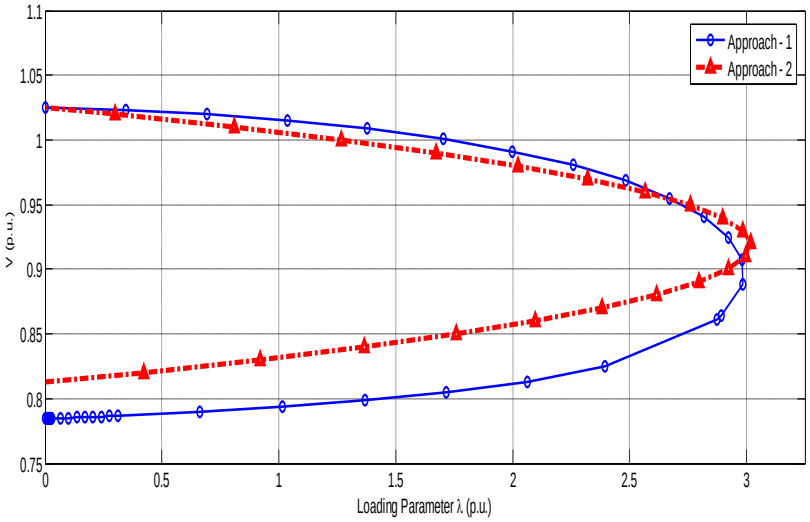

Figure 3.3: Nose curve of critical bus 4 under line outage 2-3 for *k* = 1.0 (IEEE 14-bus system)

3.3.2. New England 39-Bus System

λ-V curve of all the load buses were obtained using Approach-1 and Approach-2, respectively. Phasor measurements were obtained using optimally placed 21 PMUs at bus numbers 4, 8, 12, 16, 18, 20, 23, 25, 26, 27, 29, 30, 31, 32, 33, 34, 35, 36, 37, 38 and 39 (as per Table 2.5).

Voltage magnitude of critical buses at the base case operating point with λ=0 (i.e. at point 1) have been shown in Table 3.15 for k=0.2, Table 3.16 for k=0.5, Table 3.17 for k=1.0 and Table 3.18 for k=1.2, respectively. Loading factor of critical buses corresponding to bus voltage magnitude of 0.95 p.u. (i.e. at point 2) have been shown in Table 3.19 for k=0.2, Table 3.20 for k=0.5, Table 3.21 for k=1.0 and in Table 3.22 for k=1.2, respectively. Loading factor of critical buses corresponding to bus voltage magnitude of 0.90 p.u. (i.e. at point 3) have been shown in Table 3.23 for k=0.2, Table 3.24 for k=0.5, Table 3.25 for k=1.0 and in Table 3.26 for k=1.2, respectively.

Constants a_1, a_2, a_3 computed by Approach-2 (based on phasor measurements at three operating points) have been shown in Table 3.27, Table 3.28, Table 3.29 and Table 3.30 for k=0.2, k=0.5, k=1.0 and k=1.2, respectively. Voltage stability margin (maximum loadability i.e. λ_{max}) obtained by two approaches have been shown in Table 3.31, Table 3.32, Table 3.33 and Table 3.34 for k=0.2, k=0.5, k=1.0 and k=1.2, respectively.

Loading factor versus bus voltage magnitude (λ-V) curve of critical bus 24 under line outage 21-22 for k=0.2, obtained by two approaches, have been shown in Figure-3.4. λ-V curve of critical bus 28 under line outage 28-29 for k=0.5, obtained by two approaches, have been shown in Figure-3.5. Loading factor versus bus voltage magnitude (λ-V) curve of critical bus 15 under line outage 15-16 for k=1.0, obtained by two approaches, have been shown in Figure-3.6. λ-V curve of critical bus 29 under line outage 29-38 for k=1.2, obtained by two approaches, have been shown in Figure-3.7.

It is observed from Table 3.31, Table 3.32, Table 3.33 and Table 3.34, and Figure-3.4, Figure-3.5, that voltage stability margin estimated by the proposed

approach of quadratic nose curve fitting using PMU measurements closely match with voltage stability margin estimated by full continuation power flow for most of the cases. However, it is observed from Figure 3.6 and Figure 3.7 that there is significant difference between λ_{max} estimated by proposed approach and full continuation power flow. This may be due to consideration of dynamics of different components in PMU measurements.

Critical contingencies as well as critical buses depend upon system dynamic conditions in case of real time systems. However, in order to compare voltage stability margin estimated by proposed approach with existing approach, critical contingencies have been obtained based on voltage stability margin (distance between the base case operating point and the nose point) computed by continuation power flow method. Critical buses have been obtained based on sensitivity of bus voltage magnitude to loading factor (i.e. $dV/d\lambda$) computed near nose point of λ-V curve. PMU measurements have been obtained using PSAT software.

Table 3.15: Voltage Magnitude of critical buses at point-1 (λ=0, k=0.2)

Line Outage	**Critical Bus No.**	**Bus Voltage Magnitude (p.u.)**
		Approach-1 & Approach-2
Intact Case	7	1.01
29-38	29	1.01
22-35	29	1.01
21-22	24	1.04
19-33	29	1.01
10-32	29	1.01
23-36	29	1.01
25-37	29	1.01
20-34	29	1.01
28-29	28	1.07
13-14	29	1.01

Table 3.16: Voltage magnitude of critical buses at point-1 (λ=0, *k*=0.5)

Line Outage	Critical Bus No.	Bus Voltage Magnitude (p.u.)
		Approach-1 & Approach-2
Intact Case	7	1.01
29-38	29	1.01
22-35	29	1.01
21-22	29	1.02
19-33	29	1.01
23-36	29	1.01
25-37	7	1.01
20-34	7	1.01
28-29	28	1.07
13-14	7	1.01

Table 3.17: Voltage magnitude of critical buses at point-1 (λ=0, *k*=1.0)

Line Outage	Critical Bus No.	Bus Voltage Magnitude (p.u.)
		Approach-1 & Approach-2
Intact Case	7	1.01
29-38	29	1.06
10-32	7	1.01
22-35	7	1.01
19-33	7	1.01
21-22	24	1.04
23-36	7	1.01
25-37	7	1.01
20-34	7	1.01
15-16	15	1.03
28-29	28	1.07

Table 3.18: Voltage magnitude of critical buses at point-1 (λ=0, k=1.2)

Line Outage	Critical Bus No.	Bus Voltage Magnitude (p.u.)
		Approach-1 & Approach-2
Intact Case	7	1.01
29-38	29	1.03
10-32	7	1.01
22-35	7	1.01
19-33	7	1.01
15-16	15	1.01
23-36	7	1.01
25-37	7	1.01
21-22	24	1.04
20-34	7	1.01
13-14	7	1.01

Table 3.19: Loading factor of critical buses at point-2 (V=0.95 p.u., k=0.2)

Line Outage	Critical Bus No.	Loading Factor
		Approach-1 & Approach-2
Intact Case	7	3.61
29-38	29	1.62
22-35	29	1.89
21-22	24	2.56
19-33	29	2.03
10-32	29	2.03
23-36	29	2.19
25-37	29	2.26
20-34	29	2.28
28-29	28	2.06
13-14	29	3.80

Table 3.20: Loading factor of critical buses at point-2 (*V*=0.95 p.u., *k*=0.5)

Line Outage	Critical Bus No.	Loading Factor
		Approach-1 & Approach-2
Intact Case	7	3.35
29-38	29	1.89
22-35	29	1.88
21-22	29	2.04
19-33	29	1.91
23-36	29	2.30
25-37	7	2.55
20-34	7	2.58
28-29	28	2.37
13-14	7	4.09

Table 3.21: Loading factor of critical buses at point-2 (*V*=0.95 p.u., *k*=1.0)

Line Outage	Critical Bus No.	Loading Factor
		Approach-1 & Approach-2
Intact Case	7	3.60
29-38	29	2.30
10-32	7	2.53
22-35	7	2.46
19-33	7	2.40
21-22	24	2.32
23-36	7	2.68
25-37	7	2.56
20-34	7	2.87
15-16	15	1.40
28-29	28	2.90

Table 3.22: Loading factor of critical buses at point-2 (*V*=0.95 p.u., *k*=1.2)

Line Outage	Critical Bus No.	Loading Factor
		Approach-1 & Approach-2
Intact Case	7	4.05
29-38	29	3.05
10-32	7	2.62
22-35	7	2.27
19-33	7	2.40
15-16	15	1.40
23-36	7	2.68
25-37	7	2.56
21-22	24	2.32
20-34	7	2.78
13-14	7	4.36

Table 3.23: Loading factor of critical buses at point-3 (*V*=0.90 p.u., *k*=0.2)

Line Outage	Critical Bus No.	Loading Factor
		Approach-1 & Approach-2
Intact Case	7	5.01
29-38	29	2.34
22-35	29	2.68
21-22	24	2.97
19-33	29	2.71
10-32	29	2.70
23-36	29	2.89
25-37	29	2.90
20-34	29	2.98
28-29	28	3.44
13-14	29	4.50

Table 3.24: Loading factor of critical buses at point-3 (*V*=0.90 p.u., *k*=0.5)

Line Outage	Critical Bus No.	Loading Factor
		Approach-1 & Approach-2
Intact Case	7	4.95
29-38	29	2.29
22-35	29	2.69
21-22	29	3.31
19-33	29	2.71
23-36	29	2.89
25-37	7	3.09
20-34	7	3.19
28-29	28	3.44
13-14	7	4.89

Table 3.25: Loading factor of critical buses at point-3 (*V*=0.90 p.u., *k*=1.0)

Line Outage	Critical Bus No.	Loading Factor
		Approach-1 & Approach-2
Intact Case	7	5.04
29-38	29	2.50
10-32	7	2.89
22-35	7	2.86
19-33	7	2.91
21-22	24	3.00
23-36	7	3.09
25-37	7	3.09
20-34	7	3.18
15-16	15	2.44
28-29	28	3.44

Table 3.26: Loading factor of critical buses at point-3 (*V*=0.90 p.u., *k*=1.2)

Line Outage	Critical Bus No.	Loading Factor
		Approach-1 & Approach-2
Intact Case	7	5.04
29-38	29	3.79
10-32	7	2.89
22-35	7	2.86
19-33	7	2.92
15-16	15	2.09
23-36	7	3.08
25-37	7	3.09
21-22	24	2.93
20-34	7	3.18
13-14	7	4.89

Table 3.27: Constants a_1, a_2, a_3 for *k*=0.2

Line Outage	Critical Bus No.	Evaluated Constants		
		a_1	a_2	a_3
		Approach-2	Approach-2	Approach-2
Intact Case	7	-21645	43034	-21385
29-38	29	-1968.8	3827.6	-1857.5
22-35	29	-2367.2	4611.8	-2243.1
21-22	24	-229.8	423.5	-192
19-33	29	-2172.2	4227.1	-2053.4
10-32	29	-1983.3	3851.1	-1866.4
23-36	29	-1991.9	3861.9	-1868.5
25-37	29	-2072.4	4026	-1952.2
20-34	29	-2160.7	4196.4	-2034.1
28-29	28	-251.3	480.2	-225.8
13-14	29	-1285.3	2442.8	-1156

Table 3.28: Constants a_1, a_2, a_3 for k=0.5

Line Outage	Critical Bus No.	Evaluated Constants		
		a_1	a_2	a_3
		Approach-2	Approach-2	Approach-2
Intact Case	7	-9985.5	1969.2	-9702.8
29-38	29	-1758.7	3425.1	-1665.3
22-35	29	-2221.8	4319.8	-2096.5
21-22	29	-26078	52282	-26200
19-33	29	-2439.2	4753.4	-2312.7
23-36	29	-1797.2	3479.5	-1680.9
25-37	7	-15019	29850	-14828
20-34	7	-15156	30115	-14956
28-29	28	-157.3	290	-130
13-14	7	-7834.6	15403	-7565.4

Table 3.29: Constants a_1, a_2, a_3 for k=1.0

Line Outage	Critical Bus No.	Evaluated Constants		
		a_1	a_2	a_3
		Approach-2	Approach-2	Approach-2
Intact Case	7	-3493.2	6752.4	-3256.6
29-38	29	-169	305.2	-133.7
10-32	7	-5301.8	10389	-5084.7
22-35	7	-5591.4	10979	-5385.2
19-33	7	-5634.7	11065	-5428.1
21-22	24	-378.7	714.7	-333.8
23-36	7	-5229.9	10251	-5018.1
25-37	7	-5371.4	10539	-5165
20-34	7	-4995.8	9779.4	-4781.1
15-16	15	-45.4	67.7	-21.6
28-29	28	-84.7	146	-59.1

Table 3.30: Constants a_1, a_2, a_3 for k=1.2

Line Outage	Critical Bus No.	Evaluated Constants		
		a_1	a_2	a_3
		Approach-2	Approach-2	Approach-2
Intact Case	7	-2455.3	4696.8	-2239.2
29-38	29	-155.4	272.3	-115.4
10-32	7	-3740.6	7278.8	-3535.8
22-35	7	-4100.7	8008	-3905
19-33	7	-3999.8	7805.1	-3803
15-16	15	-35	49.7	-14.2
23-36	7	-3692.8	7187.5	-3492.4
25-37	7	-3863.8	7534	-3668
21-22	24	-504.7	968.7	-461.8
20-34	7	-3643.5	7087.8	-3442
13-14	7	-2383.8	4565.5	-2179.4

Table 3.31: Voltage stability margin by two approaches for k = 0.2

Line outage	Critical Bus No.	Approach-1	Approach-2
Intact	7	5.07	5.36
29-38	29	2.34	2.90
22-35	29	2.69	3.13
21-22	24	2.97	3.09
19-33	29	2.73	3.05
10-32	29	2.71	3.10
23-36	29	2.89	3.35
25-37	29	2.92	3.17
20-34	29	2.99	3.35
28-29	28	3.47	3.52
13-14	29	4.53	4.65

Table 3.32: Voltage stability margin by two approaches for k = 0.5

Line outage	Critical Bus No.	Approach-1	Approach-2
Intact	7	5.07	5.67
29-38	29	2.34	2.37
22-35	29	2.69	3.26
21-22	29	3.39	3.93
19-33	29	2.73	3.17
23-36	29	2.89	3.23
25-37	7	3.12	3.88
20-34	7	3.19	4.04
28-29	28	3.47	3.62
13-14	7	4.90	5.63

Table 3.33: Voltage stability margin by two approaches for k = 1.0

Line outage	Critical Bus No.	Approach-1	Approach-2
Intact	7	5.07	6.56
29-38	29	2.50	4.15
10-32	7	2.89	4.79
22-35	7	2.88	4.40
19-33	7	2.92	4.40
21-22	24	3.00	3.32
23-36	7	3.09	4.66
25-37	7	3.12	4.46
20-34	7	3.19	4.82
15-16	15	4.52	3.61
28-29	28	3.48	3.78

Table 3.34: Voltage stability margin by two approaches for k = 1.2

Line outage	Critical Bus No.	Approach-1	Approach-2
Intact	7	5.07	6.99
29-38	29	4.82	3.88
10-32	7	2.90	5.09
22-35	7	2.88	4.58
19-33	7	2.92	4.67
15-16	15	4.13	3.43
23-36	7	3.09	4.96
25-37	7	3.12	4.70
21-22	24	3.02	3.04
20-34	7	3.19	5.04
13-14	7	4.90	6.51

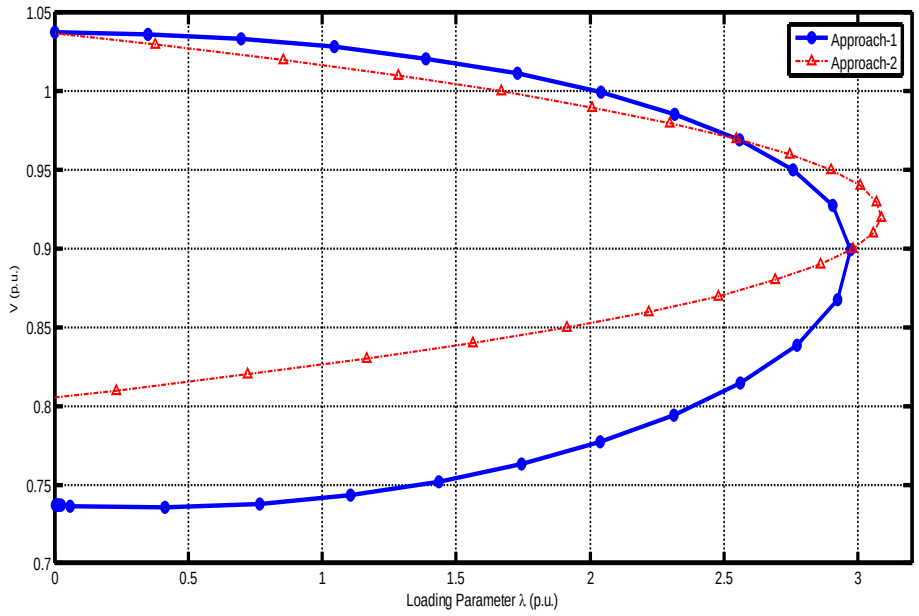

Figure 3.4: Nose curve of critical bus 24 under line outage 21-22 for k = 0.2 (New England 39-bus system)

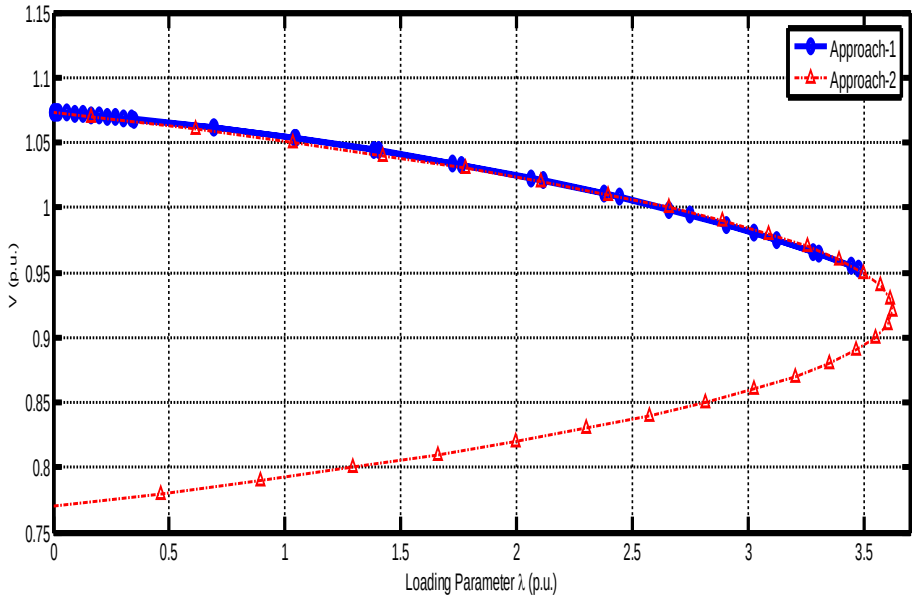

Figure 3.5: Nose curve of critical bus 28 under line outage 28-29 for *k* = 0.5 (New England 39-bus system)

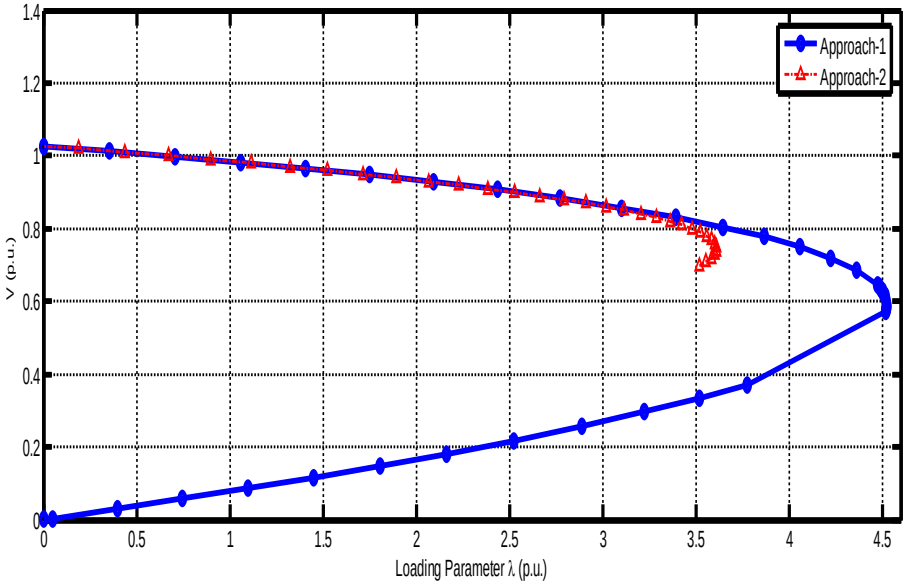

Figure 3.6: Nose curve of critical bus 15 under line outage 15-16 for *k* = 1.0 (New England 39-bus system)

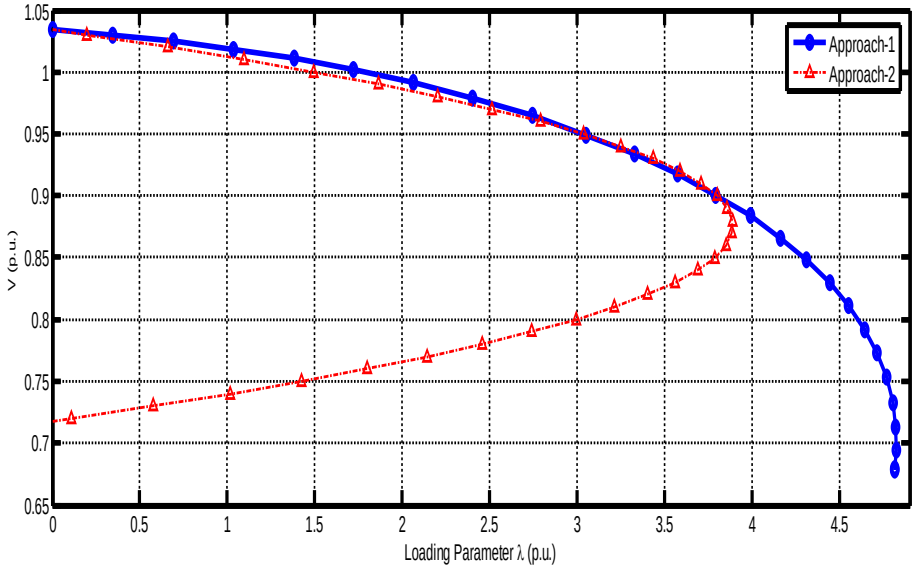

Figure 3.7: Nose curve of critical bus 29 under line outage 29-38 for *k* = 1.2 (New England 39-bus system)

3.3.3 Indian 246-Bus Northern Region Power Grid (NRPG) System

PMUs have been optimally placed using Binary Integer Linear Programming (BILP). It requires 97 PMUs (as per Table 2.8) with total observability index of 419 to ensure complete observability of the system. Nose curves were estimated by two approaches (viz. full continuation power flow and quadratic fitting of nose curves based on phasor measurements).

Voltage magnitude of critical buses at the base case operating point with λ=0 (i.e. at point 1) have been shown in Table 3.35 for *k*=0.2, Table 3.36 for *k*=0.5, Table 3.37 for *k*=1.0 and Table 3.38 for *k*=1.2, respectively. Loading factor of critical buses corresponding to bus voltage magnitude of 0.95 p.u. (i.e. at point 2) have been shown in Table 3.39 for *k*=0.2, Table 3.40 for *k*=0.5, Table 3.41 for *k*=1.0 and in Table 3.42 for *k*=1.2, respectively. Loading factor of critical buses corresponding to bus voltage

magnitude of 0.90 p.u. (i.e. at point 3) have been shown in Table 3.43 for k=0.2, Table 3.44 for k=0.5, Table 3.45 for k=1.0 and in Table 3.46 for k=1.2, respectively.

Constants a_1, a_2, a_3 computed by Approach-2 (based on phasor measurements) have been shown in Table 3.47, Table 3.48, Table 3.49 and Table 3.50 for k=0.2, k=0.5, k=1.0 and k=1.2, respectively. Voltage stability margin (maximum loadability i.e. λ_{max}) obtained by two approaches have been shown in Table 3.51, Table 3.52, Table 3.53 and Table 3.54 for k=0.2, k=0.5, k=1.0 and k=1.2, respectively.

Loading factor versus bus voltage magnitude (λ-V) curve of critical bus 24 under line outage 21-22 for k=0.2, obtained by two approaches, have been shown in Figure-3.8. λ-V curve of critical bus 28 under line outage 28-29 for k=0.5, obtained by two approaches, have been shown in Figure-3.9. Loading factor versus bus voltage magnitude (λ-V) curve of critical bus 15 under line outage 15-16 for k=1.0, obtained by two approaches, have been shown in Figure-3.10. λ-V curve of critical bus 29 under line outage 29-38 for k=1.2, obtained by two approaches, have been shown in Figure-3.11.

It is observed from Table 3.51, Table 3.52, Table 3.53 and Table 3.54, and Figure-3.8, Figure-3.10, that voltage stability margin estimated by the proposed approach of quadratic nose curve fitting by PMU measurements closely match with voltage stability margin estimated by full continuation power flow, for most of the cases. However, it is observed from Figure-3.9 and Figure-3.11 that proposed approach of voltage stability margin estimation based on quadratic fitting of nose curves using PMU measurements results in quite different loading margins compared to voltage stability margin estimated by continuation power flow method for few cases.

This shows that static model of power system assumed for running continuation power flow is not valid for real time systems. Dynamics of components such as induction motors, excitation systems affect bus voltages. Therefore, bus voltages computed by static approaches such as continuation power flow method may not be valid for real time systems. Bus voltages measured by PMUs may be more suitable for voltage stability assessment of real time systems.

Critical contingencies as well as critical buses depend upon system dynamic conditions in case of real time systems. However, in order to compare voltage stability margin estimated by proposed approach with existing approach, critical contingencies have been obtained based on voltage stability margin (distance between the base case operating point and the nose point) computed by continuation power flow method. Critical buses have been obtained based on sensitivity of bus voltage magnitude to loading factor (i.e. $dV/d\lambda$) computed near nose point of λ-V curve. PMU measurements have been obtained using PSAT software.

Table 3.35: Voltage magnitude of critical buses at point-1 (λ=0, k=0.2)

Line Outage	Critical Bus No.	Bus Voltage Magnitude (p.u.)
		Approach-1 & Approach-2
Intact Case	156	1.00
156-158	174	1.01
40-41	156	1.00
166-173	173	1.00
173-174	174	1.03
165-174	174	1.00
219-77	156	1.00
181-158	156	1.00
160-164	164	1.01
106-123	156	1.00
168-171	171	1.02

Table 3.36: Voltage magnitude of critical buses at point-1 (λ=0, *k*=0.5)

Line Outage	Critical Bus No.	Bus Voltage Magnitude (p.u.)
		Approach-1 & Approach-2
Intact Case	156	1.00
173-174	174	1.03
165-174	174	1.00
181-158	156	1.00
219-77	156	1.00
160-164	164	1.00
168-171	171	1.03
106-123	156	1.00
158-160	156	1.00
158-34	156	1.00

Table 3.37: Voltage magnitude of critical buses at point-1 (λ=0, *k*=1.0)

Line Outage	Critical Bus No.	Bus Voltage Magnitude (p.u.)
		Approach-1 & Approach-2
Intact Case	156	1.00
156-158	174	1.01
173-174	174	1.03
40-41	174	1.01
165-174	174	1.00
181-158	156	1.00
160-164	164	1.00
168-171	171	1.02
219-77	174	1.01
165-171	171	1.01

106-123	174	1.01

Table 3.38: Voltage magnitude of critical buses at point-1 (λ=0, *k*=1.2)

Line Outage	**Critical Bus No.**	**Bus Voltage Magnitude (p.u.)**
		Approach-1 & Approach-2
Intact Case	174	1.01
156-158	174	1.01
165-174	174	1.00
40-41	174	1.01
181-158	156	1.00
160-164	164	1.00
168-171	171	1.02
219-77	174	1.01
158-160	156	1.00
165-171	171	1.01

Table 3.39: Loading factor of critical buses at point-2 (*V*=0.95 p.u., *k*=0.2)

Line Outage	**Critical Bus No.**	**Loading Factor**
		Approach-1 & Approach-2
Intact Case	156	2.15
156-158	174	1.20
40-41	156	1.95
166-173	173	1.51
173-174	174	0.63
165-174	174	1.47
219-77	156	2.20
181-158	156	1.64
160-164	164	2.16

106-123	156	1.82
168-171	171	0.79

Table 3.40: Loading factor of critical buses at point-2 (*V*=0.95 p.u., *k*=0.5)

Line Outage	Critical Bus No.	Loading Factor
		Approach-1 & Approach-2
Intact Case	156	2.55
173-174	174	0.47
165-174	174	1.15
181-158	156	0.47
219-77	156	0.46
160-164	164	1.84
168-171	171	0.64
106-123	156	1.63
158-160	156	2.00
158-34	156	1.89

Table 3.41: Loading factor of critical buses at point-2 (*V*=0.95 p.u., *k*=1.0)

Line Outage	Critical Bus No.	Loading Factor
		Approach-1 & Approach-2
Intact Case	156	1.87
156-158	174	1.05
173-174	174	0.38
40-41	174	1.11
165-174	174	0.79
181-158	156	1.28
160-164	164	1.45

168-171	171	0.46
219-77	174	1.14
165-171	171	0.79
106-123	174	1.10

Table 3.42: Loading factor of critical buses at point-2 (*V*=0.95 p.u., *k*=1.2)

Line Outage	**Critical Bus No.**	**Loading Factor**
		Approach-1 & Approach-2
Intact Case	174	0.64
156-158	174	0.64
165-174	174	0.47
40-41	174	0.65
181-158	156	1.82
160-164	164	1.33
168-171	171	0.47
219-77	174	0.62
158-160	156	1.92
165-171	171	0.71

Table 3.43: Loading factor of critical buses at point-3 (*V*=0.90 p.u., *k*=0.2)

Line Outage	**Critical Bus No.**	**Loading Factor**
		Approach-1 & Approach-2
Intact Case	156	2.69
156-158	174	1.65
40-41	156	2.36
166-173	173	2.09
173-174	174	0.87
165-174	174	2.35

219-77	156	2.67
181-158	156	2.24
160-164	164	2.64
106-123	156	2.69
168-171	171	1.15

Table 3.44: Loading factor of critical buses at point-3 (*V*=0.90 p.u., *k*=0.5)

Line Outage	**Critical Bus No.**	**Loading Factor**
		Approach-1 & Approach-2
Intact Case	156	2.65
173-174	174	0.72
165-174	174	1.90
181-158	156	2.64
219-77	156	2.30
160-164	164	2.69
168-171	171	0.94
106-123	156	2.37
158-160	156	2.72
158-34	156	2.66

Table 3.45: Loading factor of critical buses at point-3 (*V*=0.90 p.u., *k*=1.0)

Line Outage	Critical Bus No.	Loading Factor
		Approach-1 & Approach-2
Intact Case	156	2.69
156-158	174	1.66
173-174	174	0.55
40-41	174	1.88
165-174	174	1.41
181-158	156	2.21

160-164	164	2.55
168-171	171	0.79
219-77	174	1.88
165-171	171	1.34
106-123	174	1.87

Table 3.46: Loading factor of critical buses at point-3 (*V*=0.90 p.u., *k*=1.2)

Line Outage	**Critical Bus No.**	**Loading Factor**
		Approach-1 & Approach-2
Intact Case	174	1.09
156-158	174	1.09
165-174	174	0.79
40-41	174	1.09
181-158	156	2.68
160-164	164	2.32
168-171	171	0.72
219-77	174	1.05
158-160	156	2.66
165-171	171	1.22

Table 3.47: Constants a_1, a_2, a_3 for *k*=0.2

Line Outage	**Critical Bus No.**	**Evaluated Constants**		
		a_1	a_2	a_3
		Approach-2	**Approach-2**	**Approach-2**
Intact Case	156	-302.1	537.3	-235.1
156-158	174	-221	400	-178.8
40-41	156	-332.5	597.1	-264.4
166-173	173	-783.7	1438.7	-654.5
173-174	174	-27.7	46.4	-18.4

165-174	174	-102.2	171.5	-69.1
219-77	156	-300.5	534.3	-233.6
181-158	156	-358.9	648.9	-289.8
160-164	164	-222.4	388.3	-165.6
106-123	156	-319.9	572	-252
168-171	171	-37.6	63.2	-25.2

Table 3.48: Constants a_1, a_2, a_3 for k=0.5

Line Outage	**Critical Bus No.**	**Evaluated Constants**		
		a_1	a_2	a_3
		Approach-2	**Approach-2**	**Approach-2**
Intact Case	156	-277.4	473	-195.4
173-174	174	-17.5	28	-10.2
165-174	174	-60.3	96.1	-35.6
181-158	156	-318.5	553.9	-235.1
219-77	156	-327.3	571.5	-243.9
160-164	164	-121.5	200.1	-78.3
168-171	171	-25.3	40.9	-15.3
106-123	156	-297.5	512.6	-214.9
158-160	156	-365.1	643.3	-278.1
158-34	156	-289.3	496.4	-206.9

Table 3.49: Constants a_1, a_2, a_3 for k=1.0

Line Outage	**Critical Bus No.**	**Evaluated Constants**		
		a_1	a_2	a_3
		Approach-2	**Approach-2**	**Approach-2**
Intact Case	156	-114.1	185.3	-71
156-158	174	-46.8	72	-25
173-174	174	-9.1	13.2	-3.9
40-41	174	-44.8	68.2	-23.1
165-174	174	-30.5	44.1	-13.5

181-158	156	-128.6	213.5	-84.8
160-164	164	-60	89.7	-29.5
168-171	171	-13.9	20.6	-6.5
219-77	174	-44.5	67.6	-22.9
165-171	171	-31.4	46.7	-15.2
106-123	174	-44.8	68.2	-23.1

Table 3.50: Constants a_1, a_2, a_3 for k=1.2

Line Outage	**Critical Bus No.**	**Evaluated Constants**		
		a_1	a_2	a_3
		Approach-2	**Approach-2**	**Approach-2**
Intact Case	174	-24.9	37.5	-12.4
156-158	174	-24.9	37.5	-12.4
165-174	174	-17.4	25.2	-7.7
40-41	174	-24.9	37.4	-12.4
181-158	156	-97.8	145.1	-47.1
160-164	164	-49.1	71	-21.8
168-171	171	-11.3	16.3	-4.7
219-77	174	-25.3	38.2	-12.8
158-160	156	-97.5	144.6	-46.9
165-171	171	-25.6	36.8	-11.1

Table 3.51: Voltage stability margin by two approaches for k = 0.2

Line outage	**Critical Bus No.**	**Approach-1**	**Approach-2**
Intact	156	2.79	3.84
156-158	174	1.73	2.35
40-41	156	2.47	3.61
166-173	173	2.09	5.67
173-174	174	1.33	1.00

165-174	174	2.76	2.76
219-77	156	2.73	3.85
181-158	156	2.26	3.45
160-164	164	2.74	3.83
106-123	156	2.78	3.72
168-171	171	1.73	1.30

Table 3.52: Voltage stability margin by two approaches for *k* = 0.5

Line outage	Critical Bus No.	Approach-1	Approach-2
Intact	156	2.78	6.21
173-174	174	1.21	0.92
165-174	174	2.77	2.59
181-158	156	2.77	5.60
219-77	156	2.36	5.46
160-164	164	2.75	3.97
168-171	171	1.59	1.19
106-123	156	2.43	5.88
158-160	156	2.78	5.27
158-34	156	2.75	6.01

Table 3.53: Voltage stability margin by two approaches for *k* = 1.0

Line outage	Critical Bus No.	Approach-1	Approach-2
Intact	156	2.78	4.14
156-158	174	1.73	2.68
173-174	174	1.03	0.84
40-41	174	2.47	2.77

165-174	174	2.75	2.40
181-158	156	2.25	3.81
160-164	164	2.74	3.97
168-171	171	1.38	1.11
219-77	174	2.73	2.78
165-171	171	2.75	2.16
106-123	174	2.78	2.77

Table 3.54: Voltage stability margin by two approaches for k = 1.2

Line outage	Critical Bus No.	Approach-1	Approach-2
Intact	174	2.17	1.64
156-158	174	2.17	1.64
165-174	174	1.74	1.37
40-41	174	2.17	1.65
181-158	156	2.77	6.64
160-164	164	2.73	3.87
168-171	171	1.30	1.08
219-77	174	2.17	1.63
158-160	156	2.78	6.65
165-171	171	2.71	2.10

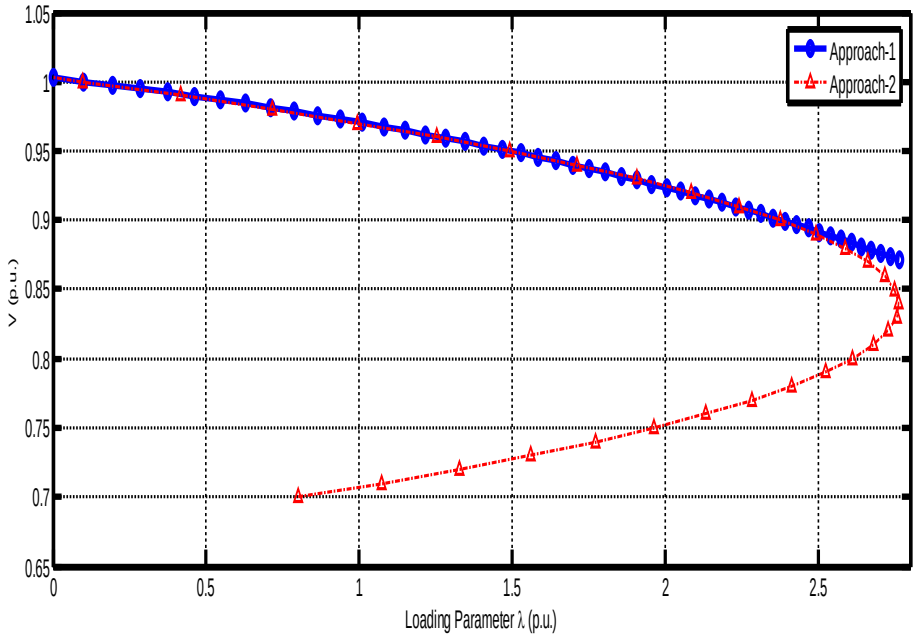

Figure 3.8: Nose curve of critical bus 174 under line outage 165-174 for *k* = 0.2 (NRPG 246-bus system)

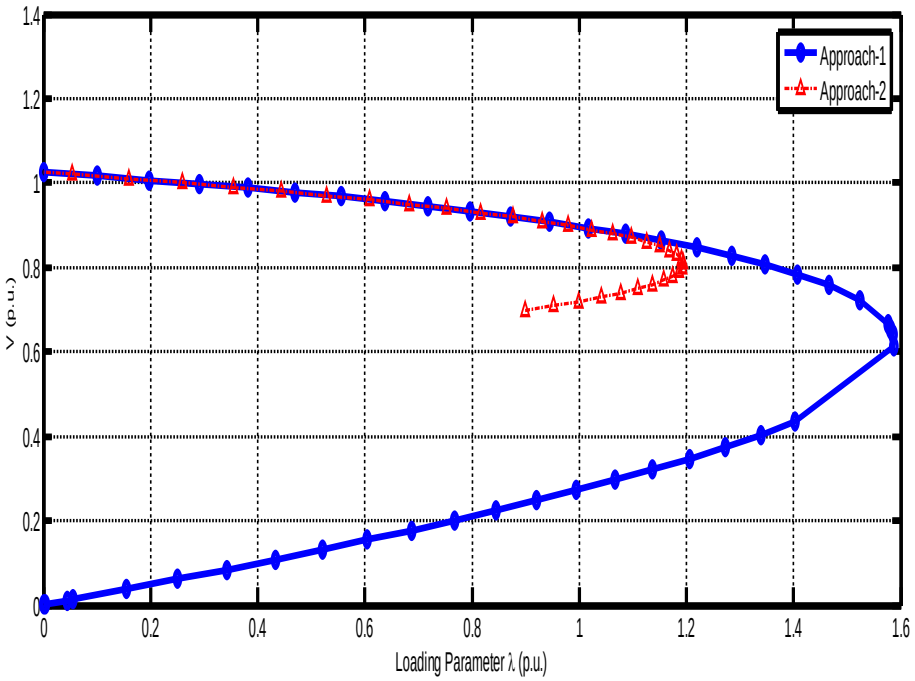

Figure 3.9: Nose curve of critical bus 171 under line outage 168-171 for *k* = 0.5 (NRPG 246-bus system)

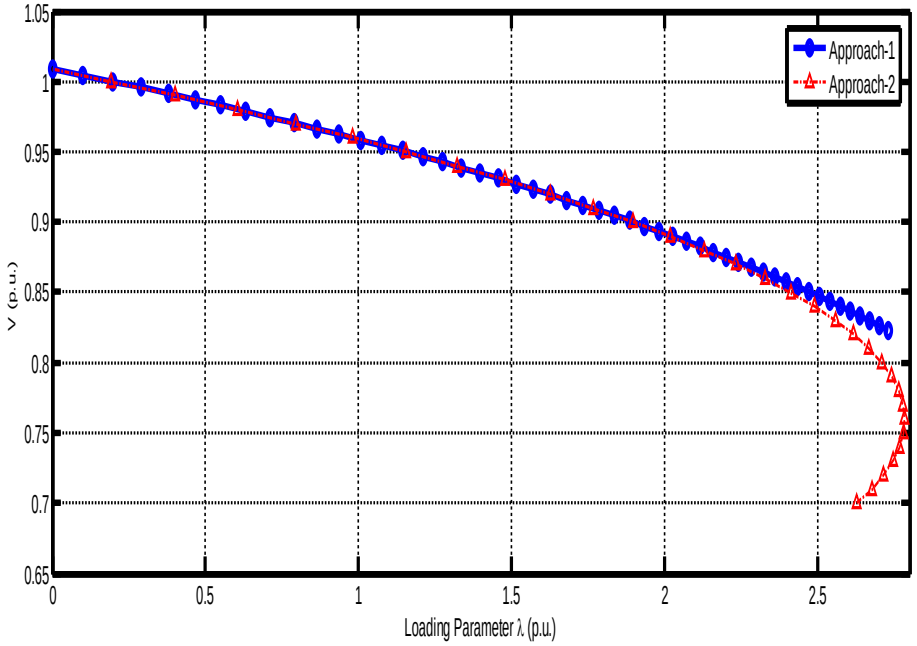

Figure 3.10: Nose curve of critical bus 174 under line outage 219-77 for *k* = 1.0 (NRPG 246-bus system)

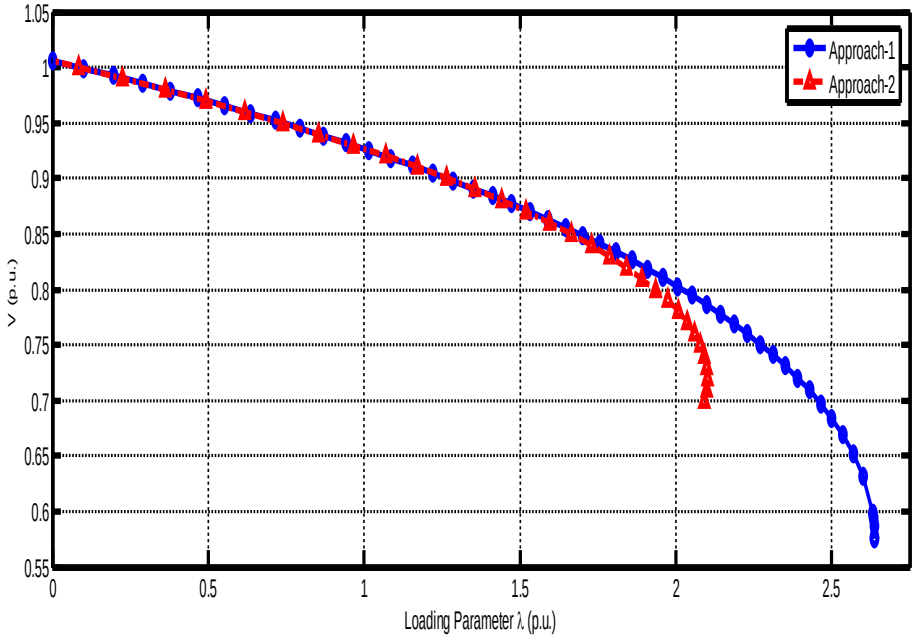

Figure 3.11: Nose curve of critical bus 171 under line outage 165-171 for *k* = 1.2 (NRPG 246-bus system)

4. Conclusions

In this chapter, quadratic fitting of nose curves using PMU measurements have been proposed. Nose curves estimated by proposed approach have been compared with nose curves obtained based on continuation power flow method. Maximum loadability (λ_{max}) estimated by proposed approach based on phasor measurements closely match with maximum loadability estimated by full continuation power flow for most of the cases except few cases. Proposed approach of voltage stability margin assessment based on PMU measurements is more suitable for real time systems as dynamics of power system components in determination of voltage stability margin is taken care by phasor measurements.